IEEE Access
Multidisciplinary | Rapid Review | Open Access Journal

Received November 10, 2017, accepted December 17, 2017, date of publication December 27, 2017,
date of current version February 14, 2018.

Digital Object Identifier 10.1109/ACCESS.2017.2786296

Compact Tunable Bandpass Filter With Wide Tuning Range of Centre Frequency and Bandwidth Using Short Coupled Lines

GANG ZHANG[1], YANHUI XU[2], AND XUEDAO WANG[2]
[1] School of Electrical and Automation Engineering, Nanjing Normal University China, Nanjing 210023, China
[2]Ministerial Key Laboratory of JGMT, Nanjing University of Science and Technology, Nanjing 210094, China

Corresponding author: Gang Zhang (gang_zhang@126.com)

This work was supported by the Science Research Foundation of Nanjing Normal University.

ABSTRACT A new compact microstrip tunable bandpass filter with continuous control of center frequency and bandwidth is proposed in the paper. The proposed design is based on short parallel-coupled lines, which are tuned by properly loading varactors. The structure exhibits a pair of transmission poles and one-side passband edge transmission zero that can be flexibly adjusted for required positions. A thorough theoretical analysis is derived to estimate the performance of the proposed filter and verify the initial values of design parameters. To verify the design concept, a prototype is fabricated and measured. The fabricated circuit has an extreme compact size (smaller than $0.03\lambda_g \times 0.1\lambda_g$). The simulated and measured results agree well with the derived theory, and indicate wide tunable center frequencies (0.56–1.15 GHz) and 1-dB bandwidth (65–180 MHz).

INDEX TERMS Bandpass filter, tunable filter, microstrip, parallel-coupled lines.

I. INTRODUCTION

Due to the increasing demand for new wireless services and applications, the high level of integration and the coexistence of multi-standard (MS) or multi-band operations into a single device are becoming defining trend in designing microwave filters. Corresponding to this trend, the reconfigurable/tunable filter that tune to different frequency bands instead of classical filter banks has been attracting more and more attention since it has great potential to significantly reduce the system size and complexity. To this end, various kinds of tunable filters have been designed for different purposes, such as tunable low-pass filters [1], [2], high-pass filters [3], bandstop filters [4], and bandpass filters (BPFs) [5]–[10]. Among these types, tunable BPFs are the most widely used devices in multiband or wideband systems. Usually, the tunability is realized by incorporating varactor diodes [5], [6], or micro-electro-mechanical-switches (MEMS) [7]–[10]. Other techniques, such as liquid crystal polymer (LCP) multilayer circuits [11], magneto static surface waves [12], and high-temperature superconductors [13] are also utilized.

Generally, tunable BPFs are desired to achieve either controllable bandwidth with constant centre frequency [14], [15], controllable centre frequency with constant bandwidth [16]–[20], or controllable bandwidth and centre frequency [21]–[35]. Among them, tunable BPFs with both controllable bandwidth and centre frequency are the ideal design scenario to meet the need for multifunctional transceivers. To achieve both reconfigurable bandwidth and centre frequency, comb-line filters [21], [22] are one of the most popular structures because their bandwidths are easily controlled by changing the coupling between the comb-line resonators, and their centre frequencies are controlled by loading the end of the comb-line resonators with varactor diodes. Other reconfigurable designs include using varactor-loaded short-ended stub resonators [23], loop-shaped dual-mode resonators [24], cross-shaped multiple-mode resonator [25], triangular resonator [26], or ring resonator [27], [28]. In designing reconfigurable BPFs, creating a controllable transmission zero (TZ) for high frequency selectivity is another important consideration. In [29] and [30], a dual-mode open-loop resonator was used to create a finite-frequency TZ on either side of the passband. In [31], two independently adjustable TZs were generated to separately adjust the centre frequency and bandwidth over a wide tuning range. By employing

varactor-loaded short-ended resonators, a tuned TZ was created to improve the lower band selectivity and response symmetry of a three-pole tunable BPF in [32]. Besides, a modified coupled line and a varactor-loaded stub were utilized in [33] to achieve a wide bandwidth tuning range by controlling the TZ around the lower/higher passband skirt. In addition, a new class of tunable filters have been proposed in [34] and [35], where tunable centre frequency and bandwidth, and a controllable one-side band edge TZ are all obtained by adopting a varactor-loaded T-shaped resonator and half-wavelength open-ended resonators, respectively.

By reviewing these previously published works, it can be found that although good performances were achieved in the reported works, there is still a challenge about whether one simple structure with a significantly more compact size can be utilized to achieve a wider tuning range for both of the centre frequency and bandwidth with controllable TZ. For this purpose, an innovative compact tunable BPF utilizing only a short two-pole varactor-loaded coupled line structure is proposed. A wide tuning range for both the centre frequency and bandwidth with sharp selectivity is realized. A detailed analysis and design procedure are provided to guide the filter design. To verify the design concept, one prototype is fabricated and measured. Compared with other related works, the proposed tunable filter achieves wide centre frequency tuning range from 0.56 to 1.15 GHz, bandwidth tuning range from 65 up to 180 MHz and an reconfigurable one-side band edge transmission zero, utilizing the compact planar structure. The calculated performance as well as simulated and measured results demonstrates the validity of the proposed design.

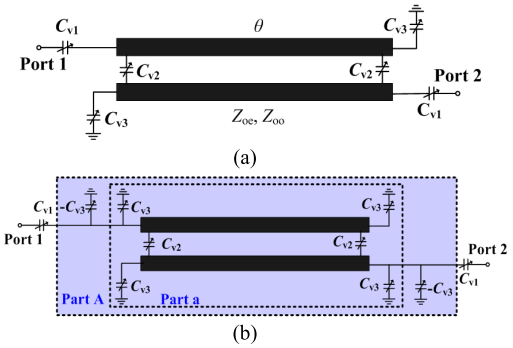

FIGURE 1. Circuit model of the proposed filter: (a) Proposed tunable BPF, (b) Transformed circuit.

II. PROPOSED FILTER AND PERFORMANCE ANALYSIS

Fig. 1*a* shows the configuration of the proposed filter. It has a simple structure that includes a short section of coupled lines with an electrical length of θ and even- and odd-mode impedances of Z_{oe} and Z_{oo} loaded with varactor diodes that have capacitances of C_{v1}, C_{v2}, and C_{v3}. Since the structure is not symmetric, a transformed circuit with two grounded capacitances C_{v3} and $-C_{v3}$ is presented in Fig. 1*b*. Those capacitances do not change the circuit characteristics from the one shown in Fig. 1*a*, but enable a simple even-/odd-mode analysis of Part a depicted in Fig. 1*b* to find its admittance-matrix following the method in [36], which can then be utilized to show that the admittance-matrix of Part A in Fig. 1*b* has the following elements.

$$Y_{11} = Y_{22} = \frac{2A_e^2A_o^2(Z_{ine}+Z_{ino})}{A_e^2A_o^2(Z_{ine}+Z_{ino})^2-(A_oZ_{ine}+A_eZ_{ino})^2} - jB_3 \quad (1)$$

$$Y_{12} = Y_{21} = \frac{2A_eA_o(A_oZ_{ine}+A_eZ_{ino})}{A_e^2A_o^2(Z_{ine}+Z_{ino})^2-(A_oZ_{ine}+A_eZ_{ino})^2} \quad (2)$$

where Z_{ine} and Z_{ino} are the even- and odd-mode input impedance seen at left or right port of Part a when the other port is open-circuited, A_e and A_o are the A-elements of the ABCD matrix of the even-/odd-mode circuits of Part a. The aforementioned parameters can be obtained from the ABCD matrices of the even-/odd-mode circuits.

$$Z_{ine} = -j\frac{Z_{oe}(1-Z_{oe}B_3\tan\theta)}{Z_{oe}B_3(2-Z_{oe}B_3\tan\theta)+\tan\theta} \quad (3)$$

$$Z_{ino} = \frac{-jZ_{oo}[1-Z_{oo}(B_3+2B_2)\tan\theta]}{Z_{oo}(B_3+2B_2)[2-Z_{oo}(B_3+2B_2)\tan\theta]+\tan\theta} \quad (4)$$

$$A_e = \cos\theta(1-Z_{oe}B_3\tan\theta) \quad (5)$$

$$A_o = \cos\theta[1-Z_{oo}\omega(B_3+2B_2)\tan\theta] \quad (6)$$

$$B_1 = \omega C_{v1}, \quad B_2 = \omega C_{v2}, \quad B_3 = \omega C_{v3} \quad (7)$$

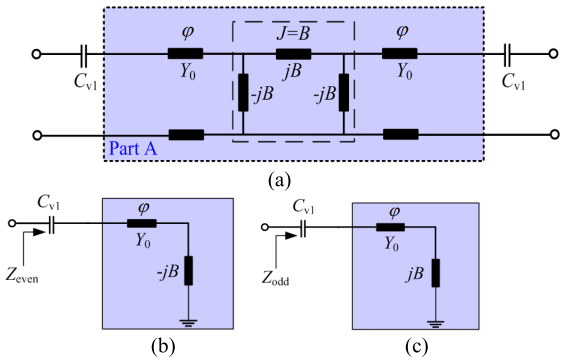

FIGURE 2. Equivalent circuits of the proposed tunable filter: (a) Equivalent J-inverter topology of the proposed tunable filter, (b) Even-mode bisection, (c) Odd-mode bisection.

To investigate the performance of the proposed tunable filter, an admittance π-model can be derived based on the obtained Y-matrix of Part A indicated in Fig. 1*b*, and further simplified into a susceptance π-model if the lossless case is assumed [37]. Considering Part A being rotationally symmetric, it can be transformed to a J-inverter topology that includes a susceptance and two transmission lines (i.e. Y_0, φ) [38] as shown in Part a of Fig. 2*a*. The values of the parameters used in Fig. 2 can be derived from:

$$\bar{J} = \frac{J}{\sqrt{Y_0^2}} = \frac{\sin(-\varphi)+\overline{B_{11}}\cos(-\varphi)}{\overline{B_{12}}\sin(-\varphi)} \quad (8)$$

$$\varphi = (M\pi + \tan^{-1}\left(\frac{2(\overline{B_{11}}+\overline{B_{22}}\,|\bar{B}|)}{1+\overline{B_{22}}^2-\overline{B_{11}}^2-|\bar{B}|^2}\right))/2 \quad (9)$$

where, $\overline{B_{11}} = \frac{Im(Y_{11})}{Y_0}, \overline{B_{22}} = \frac{Im(Y_{22})}{Y_0}, \overline{B_{12}} = \frac{Im(Y_{12})}{Y_0^2}$, and $|\bar{B}| = \overline{B_{11}B_{22}} - \overline{B_{12}}^2$. M are positive integers and $\bar{J}$ is the normalized J-inverter susceptance.

Using the equivalent circuit models under even-/odd-mode operation in Fig. 2, the even- and odd-mode resonant frequencies can be derived as follows.

$$Z_{\text{even}} = \frac{1 + \bar{J}\tan\varphi}{jY_0(\tan\varphi - \bar{J})} + \frac{1}{jB_1} = 0 \tag{10}$$

$$Z_{\text{odd}} = \frac{1 - \bar{J}\tan\varphi}{jY_0(\tan\varphi + \bar{J})} + \frac{1}{jB_1} = 0 \tag{11}$$

The conventional root-finding algorithm can be used to solve (10) and (11) in Matlab. The obtained results for the even- and odd-mode resonant frequencies (f_{even}, f_{odd}) are depicted in Fig. 3 for different values of C_{v1}, C_{v2}, and C_{v3}.

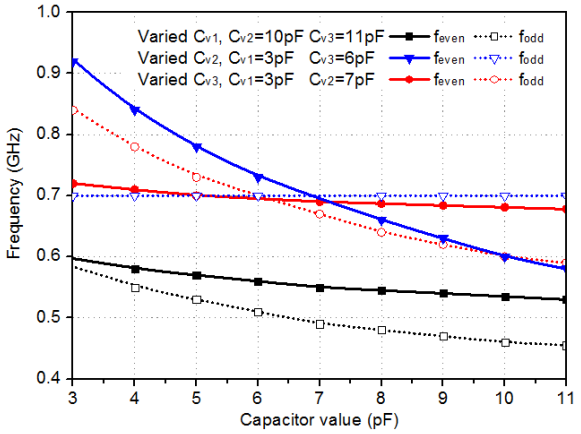

FIGURE 3. Variation of the resonant frequencies with C_{v1}, C_{v2}, and C_{v3} ($Z_{oe} = 185\ \Omega$, $Z_{oo} = 45\ \Omega$, and length of the coupled line structure equals to one-tenth wavelength at 0.8 GHz).

As shown in Fig. 3, f_{even} and f_{odd} of the whole structure decrease as C_{v1} increases. In fact, C_{v1} mainly provides the required external quality factor and only alters the even- and odd-mode frequencies by a relatively small amount compared with the effect of C_{v2} and C_{v3} as indicated in Fig. 3. In other words, f_{even} and f_{odd} are mainly determined by C_{v2} and C_{v3}. It is observed that C_{v2} can be used to significantly change f_{even} with limited effect on f_{odd}, while changing C_{v3} causes a significant variation in f_{odd} and limited effect on f_{even}. Thus, the upper (or lower) passband edges, which are determined by the position of f_{even} (or f_{odd}), can be tuned by C_{v2} (or C_{v3}) when a fixed value of C_{v1} is given, indicating a potential of bandwidth tunability. On the other hand, those two resonant frequencies can be moved to lower and higher frequencies at the same time when appropriate values for C_{v2} and C_{v3} are given with certain value for C_{v1}, and this indicates a potential centre frequency tunability.

The transmission zero (TZ) of the proposed filter can be obtained by solving the following equation,

$$\frac{Z_{\text{ine}}}{A_{\text{e}}} = \frac{Z_{\text{ino}}}{A_{\text{o}}} \tag{12}$$

Using (3) - (7), this relation can be written as,

$$\tan\theta_{\text{TZ}} = \frac{4B_2}{Z_{\text{oo}}(2B_2 + B_3)^2 - Z_{\text{oe}}B_3^2 + (Y_{\text{oe}} - Y_{\text{oo}})} \tag{13}$$

From (13), it is found that the location of the TZ is not affected by C_{v1}, but by the capacitances C_{v2} and C_{v3}. The TZ can be found from (13) by a conventional root-finding algorithm for a given $C_{\text{v2}}/C_{\text{v3}}$. Fig. 4 shows the calculated TZ frequency f_{TZ} versus C_{v2} and C_{v3}. f_{TZ} moves to lower values as C_{v2} increases or C_{v3} decreases. It is also observed that when $f_{\text{even}} > f_{\text{odd}}$, f_{TZ} always locates at upper stopband; when $f_{\text{even}} < f_{\text{odd}}$, f_{TZ} always locates at the lower stopband. In fact, f_{TZ} can not only be located at the low or high side of the passband, but also be created within the passband.

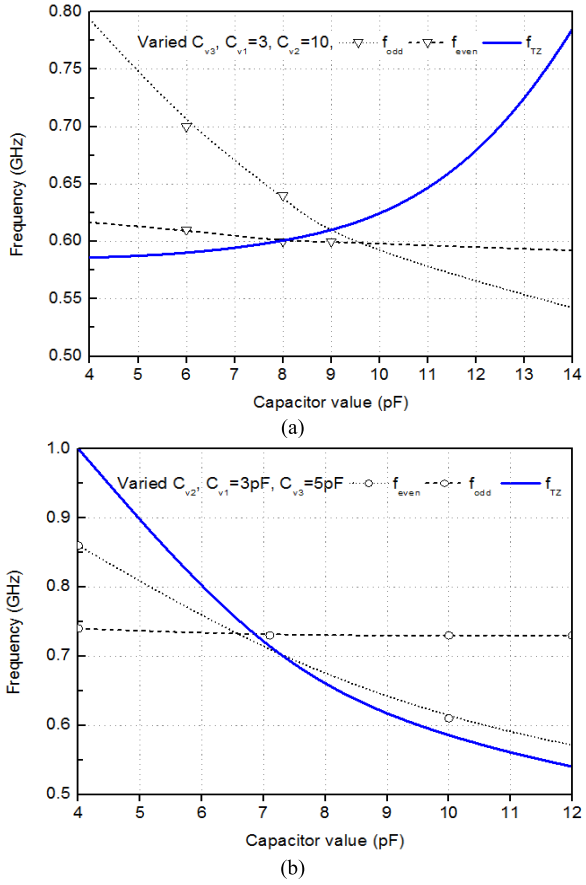

FIGURE 4. Transmission zero frequency versus the capacitances of C_{v2} and C_{v3}, (a) C_{v2} is variable, (b) C_{v3} is variable.

To determine the design parameters, the specifications for the proposed filter should be prescribed. Herein, centre frequency tuning range from 0.5 to 1.1 GHz and bandwidth tuning range from 60 to 230 MHz of the filter are set as an example. Utilizing the iterative solution based on the previous theory, it is possible to find that the following required design parameters: $Z_{\text{oe}} = 185\ \Omega$, $Z_{\text{oo}} = 45\ \Omega$, and length of the coupled structure equals to one-tenth wavelength at 0.8 GHz. According to the above analysis,

TABLE 1. Capacitances (pF) of varactors in investigated cases.

Case #	C_{v1}	C_{v2}	C_{v3}
1	1.3	5.1	6.7
2	3	3.7	6.7
3	1.4	6.4	5.8
4	2.4	6.6	4
5	3.7	12.9	19.6
6	1.5	5	6.6
7	0.8	2.6	3.2
8	2.9	17.4	15.8
9	1.2	6.3	6
10	0.6	3.1	3

the performance of the filter can be calculated with the reasonable values of varactor capacitances given in Table 1 as shown in Fig. 5. Fig. 5*a* shows that the bandwidth can be tuned from 60 to 230 MHz using C_{v1} and C_{v2}, Fig. 5*b* shows the bandwidth tunability with a re-locatable transmission zero (TZ) from one side of the passband to the other. Figs. 5*c* and *d* indicate that the centre frequency can be tuned from 0.5 to 1.1 GHz with reconfigurable TZ at the lower/upper passband edge under a certain bandwidth.

To achieve sharper frequency selectivity and better stopband rejection, the tunable filter can be extended to higher-order by adding additional varactor loaded transmission lines with equal length between the coupled lines, which will introduce more TZs and poles. For n-order ($n \geq 3$) tunable filter design, n-2 lines can be added between the original two coupled lines to form the n coupled lines structure, which brings n-2 additional poles in the passband. Since controllable poles are required for tuning passband, one ends of the n coupled lines all still need to be loaded with varactors. Between each adjacent two coupled lines, it is still necessary to add varactors. Cv1 keeps the same way as the two-order filter. By this way, n-order tunable filter based n coupled lines structure can be easily constructed. Herein, a third-order tunable filter is developed for an example as shown in Fig. 6. Since the structure is symmetric and nonadjacent coupling is weak, the even-/odd-mode method can be approximately applied to analyze it. Considering the insertion loss mainly caused by the parasitic resistors of the varactors, the values of the resistors are all assumed as 1 ohm in the design for convenience. Fig. 7a indicates the centre frequency tunability with a wide tuning range. Three tunable TZs can be observed clearly outside the passband. As indicated in Fig. 7a, to move the centre frequency to higher values while maintaining the bandwidth unchanged, C_{v1}, C_{v2}, C_{v3} and C_{v4} should be decreased. On the other hand, Fig. 7b demonstrates a wide tuning range for the bandwidth. It can be seen from Fig. 7b, to fix the centre frequency and increase the bandwidth, C_{v1} and C_{v4} should be increased, whereas, C_{v2} and C_{v3} should be decreased. As this paper is mainly aimed to design a second-order tunable filter, the next section will give its detailed design procedure as well as experimental verification.

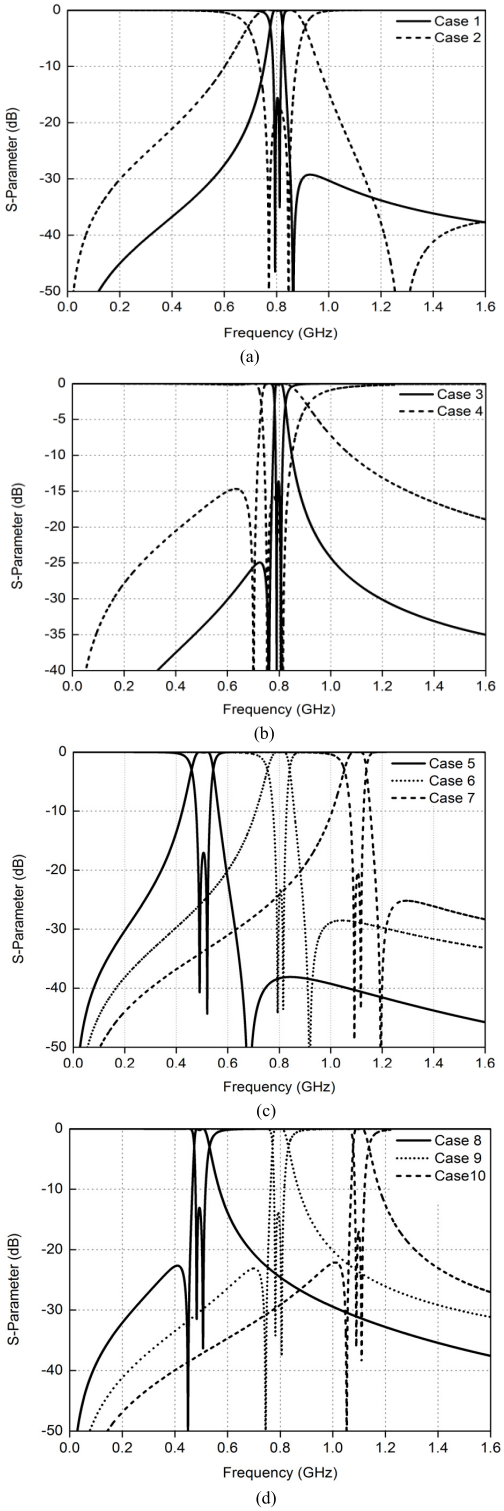

FIGURE 5. Bandwidth and centre operation frequency tunability at 0.8 GHz: (a) Bandwidth tunability when the TZ is located at upper edge of the passband, (b) Bandwidth tunability when the TZ is located at lower edge of the passband, (c) Centre operation frequency tunability when the TZ is located at upper edge of the passband, (d) Centre frequency tunability when the TZ is located at lower edge of the passband.

III. Prototype Design

Based on the explained theory, the design procedure of the proposed filter can be summarized as:

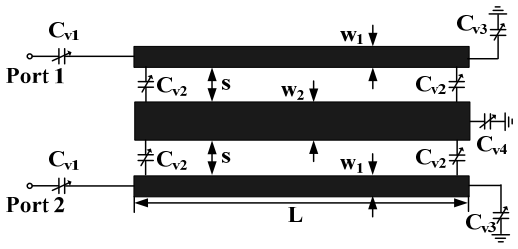

FIGURE 6. Proposed third-order tunable filter ($w_1 = w_2/2$=0.4mm, s=0.2mm and L=14.14mm; substrate RT/Duriod 6010 with $\varepsilon_r = 10.2$ and h=1.27 mm.

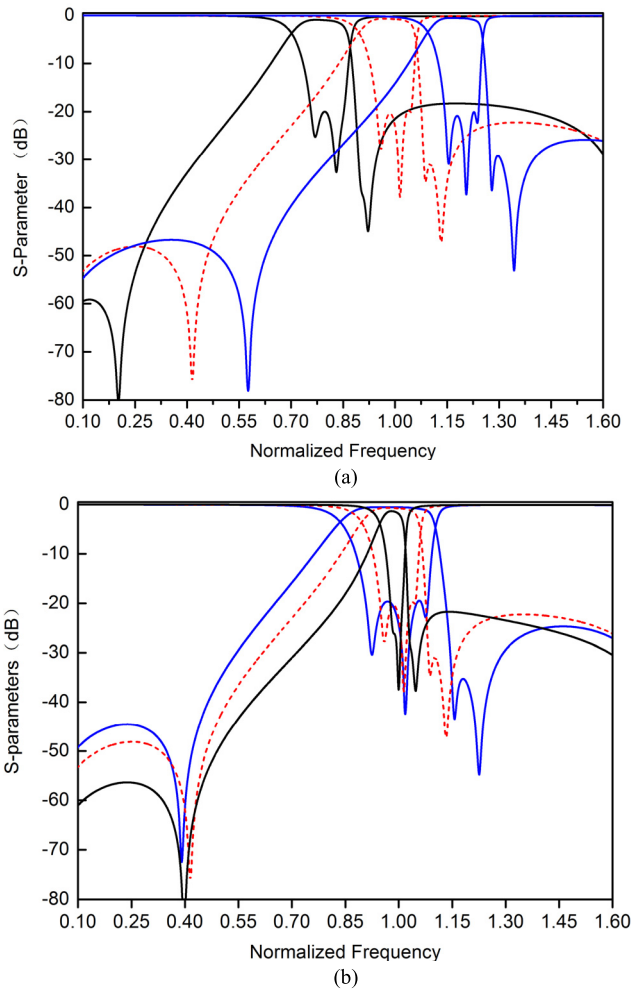

FIGURE 7. Performance of the filter with different centre frequencies and bandwidths: (a) Different centre frequencies. Biasing voltages for low frequency: C_{v1}=0.89, C_{v2}=0.6, C_{v3}=1.3, C_{v4}=9.0; middle frequency: C_{v1}=0.65, C_{v2}=0.43, C_{v3}=0.51, C_{v4}=2; high frequency: C_{v1}=0.48, C_{v2}=0.28, C_{v3}=0.2, C_{v4}=0.85. Unit: pF, (b) Different bandwidths. Narrow bandwidth: C_{v1}=0.39, C_{v2}=0.5, C_{v3}=0.73, C_{v4}=1.8; medium bandwidth: C_{v1}=0.65, C_{v2}=0.43, C_{v3}=0.51, C_{v4}=2; wide bandwidth: C_{v1}=0.96, C_{v2}=0.35, C_{v3}=0.42, C_{v4}=2.53. Unit: pF.

Step 1) Select the prototype low-pass filter, where the basic element values (g_i, $i = 0, \ldots, 3$) are known. Determine the objective centre frequency f_c and bandwidth. Based on the required fractional bandwidth FBW; calculate the desired external quality factor Q_{ext} and coupling coefficient k. Once k is known, two solutions for the even-and odd-mode resonances ($f_{even} > f_{odd}$, and $f_{even} < f_{odd}$) can be specified from (15).

$$Q_{ext} = \frac{g_0 g_1}{FBW} \tag{14}$$

$$k = \frac{|f_{even} - f_{odd}|}{f_c} = \frac{FBW}{g_1 g_2} \tag{15}$$

Step 2) Values of (Z_{oe}, Z_{oo}) are found using (26) in [19] such that the coupling coefficient of the coupled resonators can satisfy the bandwidth requirement according to (15) at the lowest frequency state. This step requires the assumption of certain maximum values C_{v1-max}, C_{v2-max}, C_{v3-max} (based on the available or selected varactors). It may results in several possible solutions. Solutions with moderate values for the mode impedances, which enable easy or low-cost fabrication, are usually selected. Using the approach in [39], determine the initial dimensions of the coupled lines from Z_{oe}, Z_{oo}.

Step 3) A conventional iterative algorithm can be used to solve (10) and (11) to find the range of values needed for C_{v1}, C_{v2}, C_{v3} to cover the required tunable range for the centre frequency and band. To this end, an initial guess for C_{v1} which should be less than C_{v1-max} is needed to solve (10) and (11) to determine C_{v2} and C_{v3}. Next, actual Q'_{ext} is evaluated using the well-known external Q method [40] and the initial guess of C_{v1} is updated so that actual Q'_{ext} equals desired Q_{ext} as calculated from (14).

Step 4) Verify the performance using the calculated values by first utilizing the presented theory and then using a full-wave simulator, which can also be utilized for design optimization.

As an example of the proposed filter, a prototype is designed with centre frequency tuning range from 0.6 to 1.2 GHz and bandwidth tuning range from 60 and 300 MHz. Using the design procedure, the required design parameters (Z_{oe} = 185 Ω, Z_{oo} = 45 Ω, C_{v1} = 0.9-7 pF, C_{v2} = 1.5-11 pF, C_{v3} = 1-15 pF) is possible to find. The design is implemented on the substrate RT/Duriod 6010 with ε_r = 10.2 and h = 1.27 mm with a microstrip technology. Fig. 8*a* depicts a diagram of the filter prototype, showing the biasing circuit for the varactors. It is noted that for the independent biasing requirement for C_{v1}, C_{v2}, and C_{v3}, a pair of varactors are employed in an anti-series configuration to represent C_{v2}. Moreover, C_b is used as DC block capacitor and R_b is the DC biasing resistor in addition to being a radio frequency choke (RFC). The full structure with its calculated initial dimensions is co-simulated using Ansoft HFSS v13 and ADS, which are also used for final optimization. Hyper abrupt junction tuning varactors SM1234-009L (tuning range 1.32-9.63 pF, and series resistor R_s = 0.8 Ω, SMV1281-097L (tuning range 0.69-13.30 pF, and R_s = 1.7 Ω) and SMV1235-004L (tuning range

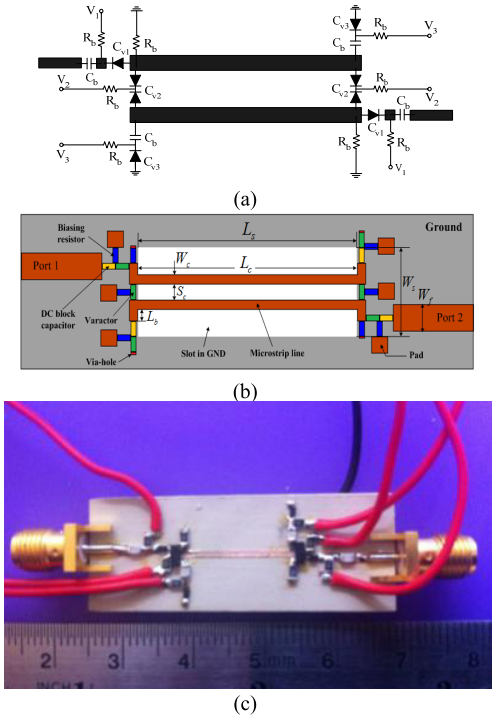

FIGURE 8. The final design: (a) Diagram of the structure with its biasing circuit, (b) Implementation using microstrip technology, (c) Fabricated filter.

2.38-18.22 pF, and $R_s = 0.6\ \Omega$), are adopted for C_{v1}, C_{v2}, and C_{v3}, respectively. Besides, Murata 0402 GRM 100 pF capacitors are used as DC block capacitors, and Panasonic resistors 100 kΩ are utilized as RFCs. For accurate simulation, SPICE models of the aforementioned varactor diodes as provided in [41] are used.

The final optimized design parameters of the tunable bandpass filter (Fig. 8*b*) were found as: $L_c = 14.6$ mm, $L_s = 14$ mm, $S_c = 0.2$ mm, $W_c = 0.4$ mm, W_f=1.21 mm and $W_s = 4.6$ mm. Herein, it is worth mentioning the grounded slot is etched on the ground layer shown in Fig. 8*b* to realize the required even- and odd-mode impedances without using the narrow gaps or thin lines in the coupled line structure [40]. Fig. 8*c* presents a photograph of the fabricated filter with a very compact size of 15 mm × 4.6 mm ($0.1\lambda_g \times 0.03\lambda_g$). The compactness is realized mainly by the variable loads at the ends of the coupled line, which has also been theoretically analyzed in [42].

Both of the simulated results and measured results are described in Figs. 9a and 9b for bandwidth tunability, Fig. 9c for centre frequency tunability, and Fig. 10 for TZ reconfigurability. Among them, Figs. 9a and 9b demonstrate tunable 1-dB bandwidth with wide tuning range from 65 to 180 MHz at low and high frequency, respectively. Fig. 9c indicates tunable centre frequency with a wide tuning range from 0.56 to 1.15 GHz. In addition, Fig. 10 shows that the reconfigurability of one-side band transmission zero is realized in the proposed design, resulting in a better cut-off at the edge of the passband. The introduced TZ can be relocated at either the lower or upper end of the passband,

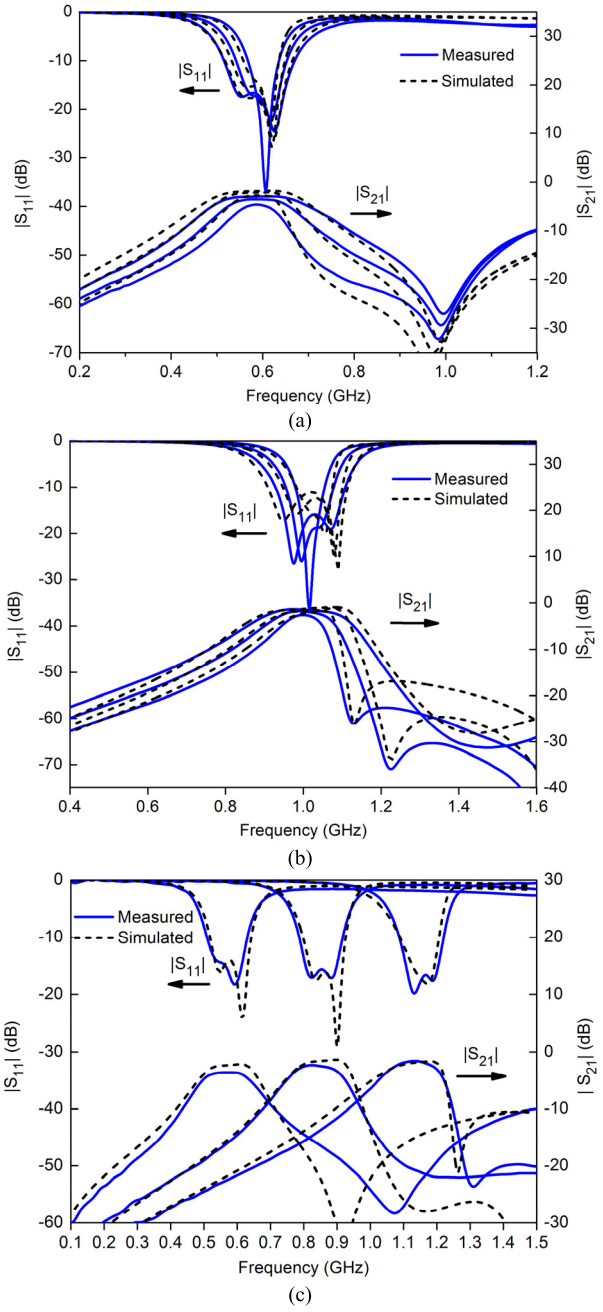

FIGURE 9. Performance of the tunable bandpass filter with different bandwidth and centre operation frequencies: (a) Different bandwidth centred at 0.58 GHz. Narrow band: V_1=3.2, V_2=0.8, V_3=1.5; medium band: V_1 = 2.0, V_2 = 1.0, V_3=1.2; wide band: V_1 = 1.3, V_2=1.1, V_3=1.1. Unit: V, (b) Different bandwidth centred at 1 GHz. Narrow band: V_1=15, V_2=6.4, V_3=10; medium band: V_1 = 12.2, V_2=7.0, V_3=9.5; wide bandwidth: V_1 = 9.9, V_2=7.8, V_3=9.0. Unit: V, (c) Different centre operation frequencies: Biasing voltages for low frequency: V_1=1.5, V_2=0, V_3=0; middle frequency: V_1=7.7, V_2=4.5, V_3=6; high frequency: V_1=15, V_2=9.9, V_3=20. Unit: V.

without affecting the passband or insertion loss. Thus, the cut-off of the passband is reconfigurable according to the different needs of realistic application. The measured insertion loss for all the investigated cases varies between 1.4 and 4.5 dB, while the return loss is more than 12 dB. Both the simulated and measured results are generally in good agreement.

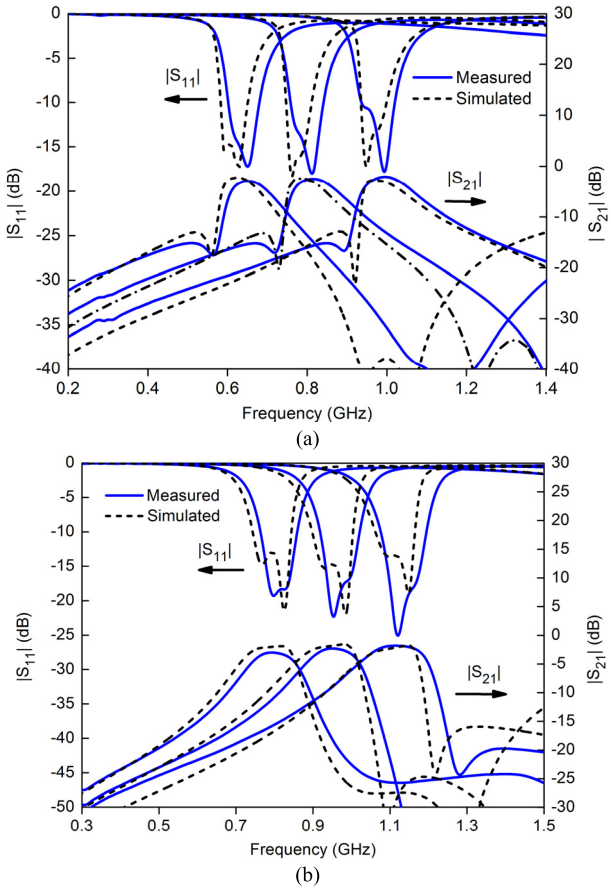

FIGURE 10. Simulated and measured results of the filter with different centre frequencies under TZ at the low/upper passband edge: (a) At the low passband edge. Biasing voltages for low frequency: V_1=4.5, V_2=0.2, V_3=3.3; middle frequency: V_1=8.8, V_2=2.1, V_3=5.8; high frequency: V_1=14.9, V_2=4.1, V_3=9.8. Unit: V, (b) At the upper passband edge. Biasing voltages for low frequency: V_1=7.9, V_2=3.3, V_3=4.7; middle frequency: V_1=11.8, V_2=5.4, V_3=7.8; high frequency: V_1=14.7, V_2=7.9, V_3=13.6. Unit: V.

It is worth mentioning that the insertion loss is due to finite quality factor (Q) of the varactor, which can be verified from a comparison of the simulations with finite Q varactor and that with an ideal capacitor (insertion loss within 1.5 dB). The finite Q introduces resistive loss to the filter. Further improvement on the insertion loss can be achieved with advanced MEMS technologies [7]. Moreover, specifically note that the quality factor of the used varactors is significantly lower than the ideal assumed value at the lower frequencies, resulting in an increased measured insertion loss at the low frequency bands. In addition, the minor discrepancies between the measured and the simulated results are caused by the higher order parasitics of the varactor, which was not completely modelled in the EM simulation.

A comparison between the proposed filter and other recent designs is given in Table 2. It is clearly shown that the presented tunable BPF exhibits the most compact size. To the best of our knowledge, there is few report on such a compact tunable filter design. Meanwhile, it also has a wider tuning range for the centre frequency with a competitive bandwidth tuning range and values of the insertion loss.

TABLE 2. Comparison of the proposed filter and otherrecent designs.

Design	Centre frequency tuning range (%)	BW tuning range (MHz){%}	Filter order	Insertion loss (dB)	Size/ ($\lambda_g \times \lambda_g$)
[22]	30	# 40-120 {300}	4	4.5~6.2	0.24×0.12
[24]	33	# 0-52	2	1.4~4.6	0.12×0.08
[26]	19	*134-402 {300}	2	1~3	0.33×0.3
[34]	49	#55-175 {318}	2	0.5~2.9	0.13×0.08
[35]	42	#115-315 {274}	2	1.2~1.5	0.43×0.12
This work	**69**	**#65-180{277}**	**2**	**1.4~4.5**	**0.1×0.03**

#: 1-dB bandwidth, *: 3-dB bandwidth.

IV. CONCLUSION

In this paper, a new compact microstrip tunable filter based on short coupled line structure has been proposed. By properly loading varactors with this compact structure, a wide tuning range for both of the centre frequency and bandwidth with reconfigurable TZ have been achieved. Based on the clear theoretical analysis, an explicit design procedure has been provided. For validation, a two-pole tunable filter has been fabricated and tested. Both the simulated and measured results exhibit a wide tuning range of the centre frequency (0.56-1.15 GHz) and the bandwidth (65-180 MHz), respectively. With the favourable properties of huge size reduction and high controllability of band coverage, it is our belief that the proposed approach is attractive for modern multiband telecommunication systems.

REFERENCES

[1] C.-C. Huang, N.-W. Chen, H.-J. Tsai, and J.-Y. Chen, "A coplanar waveguide bandwidth-tunable lowpass filter with broadband rejection," *IEEE Microw. Wireless Compon. Lett.*, vol. 23, no. 3, pp. 134–136, Mar. 2013.

[2] J. Ni and J. Hong, "Compact continuously tunable microstrip low-pass filter," *IEEE Trans. Microw. Theory Techn.*, vol. 61, no. 5, pp. 1800–1973, May 2013.

[3] J. Ni and J. Hong, "Compact varactor-tuned microstrip high-pass filter with a quasi-elliptic function response," *IEEE Trans. Microw. Theory Techn.*, vol. 61, no. 11, pp. 3853–3859, Nov. 2013.

[4] I. Reines, S.-J. Park, and G. M. Rebeiz, "Compact low-loss tunable *X*-band bandstop filter with miniature RF-MEMS switches," *IEEE Trans. Microw. Theory Techn.*, vol. 58, no. 7, pp. 1887–1895, Jul. 2010.

[5] S. R. Chandler, I. C. Hunter, and J. G. Gardiner, "Active varactor tunable bandpass filter," *IEEE Microw. Guided Wave Lett.*, vol. 3, no. 3, pp. 70–71, Mar. 1993.

[6] A. R. Brown and G. M. Rebeiz, "A varactor-tuned RF filter," *IEEE Trans. Microw. Theory Techn.*, vol. 48, no. 7, pp. 1157–1160, Jul. 2000.

[7] S.-J. Park, K.-Y. Lee, and G. M. Rebeiz, "Low-loss 5.15–5.70-GHz RF MEMS switchable filter for wireless LAN applications," *IEEE Trans. Microw. Theory Techn.*, vol. 54, no. 11, pp. 3931–3939, Nov. 2006.

[8] K. Y. Yuk, S. Fouladi, R. Ramer, and R. R. Mansour, "RF MEMS switchable interdigital bandpass filter," *IEEE Microw. Wireless Compon. Lett.*, vol. 22, no. 1, pp. 44–46, Jan. 2012.

[9] Y. Shim, Z. Wu, and M. Rais-Zadeh, "A high-performance continuously tunable MEMS bandpass filter at 1 GHz," *IEEE Trans. Microw. Theory Techn.*, vol. 60, no. 8, pp. 2439–2447, Aug. 2012.

[10] Y.-H. Cho and G. M. Rebeiz, "Two- and four-pole tunable 0.7–1.1-GHz bandpass-to-bandstop filters with bandwidth control," *IEEE Trans. Microw. Theory Techn.*, vol. 62, no. 3, pp. 457–463, Mar. 2014.

[11] A. Miller and J. Hong, "Cascaded coupled line filter with reconfigurable bandwidths using LCP multilayer circuit technology," *IEEE Trans. Microw. Theory Techn.*, vol. 60, no. 6, pp. 1577–1586, Jun. 2012.

[12] J. Wu, X. Yang, S. Beguhn, J. Lou, and N. X. Sun, "Nonreciprocal tunable low-loss bandpass filters with ultra-wideband isolation based on magnetostatic surface wave," *IEEE Trans. Microw. Theory Techn.*, vol. 6, no. 12, pp. 3959–3968, Dec. 2012.
[13] G. Suo *et al.*, "Low loss tunable superconducting dual-mode filter at L-band using semiconductor varactors," *IEEE Microw. Wireless Compon. Lett.*, vol. 24, no. 3, pp. 170–172, Mar. 2014.
[14] A. Miller and J. S. Hong, "Wideband bandpass filter with reconfigurable bandwidth," *IEEE Microw. Wireless Compon. Lett.*, vol. 20, no. 1, pp. 28–30, Jan. 2010.
[15] W.-H. Tu, "Compact low-loss reconfigurable bandpass filter with switchable bandwidth," *IEEE Microw. Wireless Compon. Lett.*, vol. 20, no. 4, pp. 208–210, Apr. 2010.
[16] S. J. Park and G. M. Rebeiz, "Low-loss two-pole tunable filters with three different predefined bandwidth characteristics," *IEEE Trans. Microw. Theory Techn.*, vol. 56, no. 5, pp. 1137–1148, May 2008.
[17] X. Y. Zhang, Q. Xue, C. H. Chan, and B.-J. Hu, "Low-loss frequency-agile bandpass filters with controllable bandwidth and suppressed second harmonic," *IEEE Trans. Microw. Theory Techn.*, vol. 58, no. 6, pp. 1557–1564, Jun. 2010.
[18] L. Athukorala and D. Budimir, "Compact second-order highly linear varactor-tuned dual-mode filters with constant bandwidth," *IEEE Trans. Microw. Theory Techn.*, vol. 59, no. 9, pp. 2214–2220, Sep. 2011.
[19] X.-G. Wang, Y.-H. Cho, and S.-W. Yun, "A tunable combline bandpass filter loaded with series resonator," *IEEE Trans. Microw. Theory Techn.*, vol. 60, no. 6, pp. 1569–1576, Jun. 2012.
[20] Q. Xiang, Q. Feng, X. Huang, and D. Jia, "Electrical tunable microstrip LC bandpass filters with constant bandwidth," *IEEE Trans. Microw. Theory Techn.*, vol. 61, no. 3, pp. 1124–1130, Mar. 2013.
[21] M. Sanchez-Renedo, "High-selectivity tunable planar combline filter with source/load-multiresonator coupling," *IEEE Microw. Wireless Compon. Lett.*, vol. 17, no. 7, pp. 513–515, Jul. 2007.
[22] Y.-C. Chiou and G. M. Rebeiz, "Tunable 1.55–2.1 GHz 4-pole elliptic bandpass filter with bandwidth control and >50 dB rejection for wireless systems," *IEEE Trans. Microw. Theory Techn.*, vol. 61, no. 1, pp. 117–124, Jan. 2013.
[23] H.-I. Baek, Y.-H. Cho, X.-G. Wang, H.-M. Lee, and S.-W. Yun, "Design of a reconfigurable active bandpass filter based on a controllable slope parameter," *IEEE Microw. Wireless Compon. Lett.*, vol. 21, no. 12, pp. 670–672, Dec. 2011.
[24] H.-J. Tsai, N.-W. Chen, and S.-K. Jeng, "Center frequency and bandwidth controllable microstrip bandpass filter design using loop-shaped dual-mode resonator," *IEEE Trans. Microw. Theory Techn.*, vol. 61, no. 10, pp. 3590–3600, Oct. 2013.
[25] J.-R. Mao, W.-W. Choi, K.-W. Tam, W. Q. Che, and Q. Xue, "Tunable bandpass filter design based on external quality factor tuning and multiple mode resonators for wideband applications," *IEEE Trans. Microw. Theory Techn.*, vol. 61, no. 7, pp. 2574–2584, Jul. 2013.
[26] A. L. C. Serrano, F. S. Correra, T.-P. Vuong, and P. Ferrari, "Synthesis methodology applied to a tunable patch filter with independent frequency and bandwidth control," *IEEE Trans. Microw. Theory Techn.*, vol. 60, no. 3, pp. 484–493, Mar. 2012.
[27] H. Zhu and A. Abbosh, "Compact tunable bandpass filter with wide tuning range using ring resonator and short-ended coupled lines," *Electron. Lett.*, vol. 51, no. 7, pp. 568–570, Apr. 2015.
[28] H. Zhu and A. Abbosh, "Compact tunable bandpass filter with wide tuning range of centre frequency and bandwidth using coupled lines and short-ended stubs," *IET Microw., Antennas Propag.*, vol. 10, no. 8, pp. 863–870, Jun. 2016.
[29] Y.-H. Chun and J.-S. Hong, "Electronically reconfigurable dual-modemicrostrip open-loop resonator filter," *IEEE Microw. Wireless Compon. Lett.*, vol. 18, no. 7, pp. 449–451, Jul. 2008.
[30] W. Tang and J.-S. Hong, "Varactor-tuned dual-mode bandpass filters," *IEEE Trans. Microw. Theory Techn.*, vol. 58, no. 8, pp. 2213–2219, Aug. 2010.
[31] J. Long, C. Li, W. Cui, J. Huangfu, and L. Ran, "A tunable microstrip bandpass filter with two independently adjustable transmission zeros," *IEEE Microw. Wireless Compon. Lett.*, vol. 21, no. 2, pp. 74–76, Feb. 2011.
[32] Y.-J. Chiou and G. M. Rebeiz, "A tunable three-pole 1.5–2.2-GHz bandpass filter with bandwidth and transmission zero control," *IEEE Trans. Microw. Theory Techn.*, vol. 59, no. 11, pp. 2872–2878, Nov. 2011.
[33] C.-W. Tang, C.-T. Tseng, and S.-C. Chang, "A tunable bandpass filter with modified parallel-coupled line," *IEEE Microw. Wireless Compon. Lett.*, vol. 23, no. 4, pp. 190–192, Apr. 2013.
[34] H.-J. Tsai, B.-C. Huang, N.-W. Chen, and S.-K. Jeng, "A reconfigurable bandpass filter based on a varactor-perturbed, T-shaped dual-mode resonator," *IEEE Microw. Wireless Compon. Lett.*, vol. 24, no. 5, pp. 297–299, May 2014.
[35] X. Luo, S. Sun, and R. B. Staszewski, "Tunable bandpass filter with two adjustable transmission poles and compensable coupling," *IEEE Trans. Microw. Theory Techn.*, vol. 62, no. 9, pp. 2003–2013, Sep. 2014.
[36] D. M. Pozar, *Microwave Engineering*, 3rd ed. New York, NY, USA: Wiley, 2005.
[37] L. Zhu and K. Wu, "Accurate circuit model of interdigital capacitor and its application to design of new quasi-lumped miniaturized filters with suppression of harmonic resonance," *IEEE Trans. Microw. Theory Techn.*, vol. 48, no. 7, pp. 353–355, Mar. 2011.
[38] R. K. Mongia, I. J. Bhartia, and J. S. Hong, *RF and Microwave Coupled-Line Circuits*, 2nd ed. New York, NY, USA: Artech House, 2007.
[39] A. M. Abbosh, "Analytical closed-form solutions for different configurations of parallel-coupled microstrip lines," *IET Microw., Antennas Propag.*, vol. 3, no. 1, pp. 137–147, Feb. 2009.
[40] J. S. Hong and M. J. Lancaster, *Microstrip Filters for RF/Microwave Applications*. New York, NY, USA: Wiley, 2001.
[41] *Skyworks SMV Datasheets*, Skyworks Solutions, Sunnyvale, CA, USA, 2011.
[42] A. M. Abbosh, "Compact tunable reflection phase shifters using short section of coupled lines," *IEEE Trans. Microw. Theory Techn.*, vol. 60, no. 8, pp. 2465–2472, 2012.

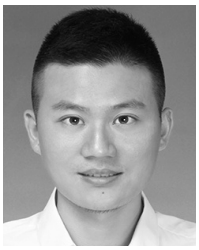

GANG ZHANG received the Ph.D. degree in electronics and information engineering from NJUST, Nanjing, China, in 2017. From 2013 to 2014, he was an Exchange Student with the School of Information Technology and Electrical Engineering, University of Queensland, Australia. He is currently with the School of Electrical and Automation Engineering, Nanjing Normal University, China. His research interests include the design of miniaturized high-performance microwave/millimeter-wave multi-function integrated passive device and numerical synthesis methods in electromagnetics.

YANHUI XU received the B.S. degree from NJUST, Nanjing, China, in 2015, where she is currently pursuing the M.Sc. degree in electromagnetic field and microwave technology. Her research interests include the high-performance microwave antenna realized on PCB.

XUEDAO WANG received the B.S. degree from NTU, Nantong, China, in 2014. She is currently pursuing the Ph.D. degree in electromagnetic field and microwave technology with NJUST, Nanjing, China. Her research interests include the design of miniaturized high-performance microwave/ millimeter-wave passive out-of-phase filtering power divider.